

Acquired Resistance to Peloruside A and Laulimalide is Associated with Downregulation of Vimentin in Human Ovarian Carcinoma Cells

Arun Kanakkanthara · Pisana Rawson · Peter T. Northcote · John H. Miller

Received: 22 February 2012 / Accepted: 30 April 2012
© Springer Science+Business Media, LLC 2012

ABSTRACT

Purpose Acquired β -tubulin alterations in human ovarian carcinoma IA9 cells were previously shown to confer resistance to the microtubule stabilizing agents peloruside A (PLA) and laulimalide (LAU). We examined the proteome of resistant cells to see what other protein changes occurred as a result of the acquired drug resistance.

Methods Two-dimensional differential in-gel electrophoresis was performed to explore differentially expressed proteins in the resistant IA9-R1 (R1) and IA9-L4 (L4) cells. The proteins on the gels were identified by MALDI-TOF MS, and altered protein abundance was confirmed by Western blotting and immunocytochemistry. Vimentin expression was restored in vimentin-deficient L4 cells by transfecting a full-length human vimentin cDNA, and sensitivity to PLA and LAU were tested using an MTT cell proliferation assay.

Results Proteomic analysis identified several proteins that were significantly altered in the resistant cells relative to the parental IA9 cells. Using Western blotting and immunocytochemistry, a decreased vimentin abundance in the L4 cells was validated. Vimentin levels were unchanged in PLA-resistant R1 cells and paclitaxel/epothilone-resistant derivatives of IA9 cells. Vimentin cDNA transfection into L4 cells partially restored PLA and LAU sensitivity.

Conclusions Downregulation of vimentin contributes to the resistance of IA9 cells to the microtubule stabilizing agents, PLA and LAU.

KEY WORDS cancer resistance · laulimalide · ovarian carcinoma cells · peloruside A · vimentin

ABBREVIATIONS

2D-DIGE	two-dimensional differential in-gel electrophoresis
BVA	biological variation analysis
DAPI	4',6-diamidino-2-phenylindole
DOX	doxorubicin
IXA	ixabepilone
LAU	laulimalide
MALDI-TOF	matrix assisted laser desorption/ionization time of flight
P-gp	P-glycoprotein
PLA	peloruside A
PTX	paclitaxel
VDP	vimentin degradation products

INTRODUCTION

Vimentin is an abundantly expressed type III intermediate filament protein. It is found primarily in cells of mesenchymal origin such as endothelial cells, fibroblasts, and smooth muscle cells and plays a major role in the epithelial-mesenchymal transition (1). Vimentin is also expressed in many cultured epithelial cells (2). It is typically expressed in the cytoplasm and interacts with a multitude of cellular proteins, including microtubules and actin microfilaments (3,4). It plays a role in several key cellular functions such as cell signaling, cell division, cell survival, apoptosis, migration, and in the regulation of intermediate filament structure and dynamics (5). There is now clear evidence that vimentin also has a role in cancer (5). For example, high abundance of vimentin in cancer cells has been linked to their increased invasiveness and metastasis, two properties crucially

A. Kanakkanthara · P. Rawson · P. T. Northcote · J. H. Miller
Centre for Biodiscovery, Victoria University of Wellington
PO Box 600, Wellington 6140, New Zealand

A. Kanakkanthara · P. Rawson · J. H. Miller (✉)
School of Biological Sciences, Victoria University of Wellington
PO Box 600, Wellington, New Zealand
e-mail: john.h.miller@vuw.ac.nz

P. T. Northcote
School of Chemical and Physical Sciences
Victoria University of Wellington
PO Box 600, Wellington, New Zealand

associated with drug resistance (6–8). Whether vimentin directly plays a role in mediating the sensitivity of cancer cells to anticancer drugs remains unclear.

Tubulin-binding agents are a successful class of drugs in the treatment of cancer (9). The development of drug resistance in cancer cells, however, often limits the clinical efficacy of these agents. A number of resistance mechanisms, such as overexpression of the P-glycoprotein (P-gp) drug efflux pump (10), alterations in tubulin structure and isotype expression (11), alterations in actin (12), and aberrant expression of microRNAs (13) have been reported previously; yet, it is obvious that several of the factors that contribute to survival of cancer cells when treated with diverse antimicrotubule agents are still to be elucidated.

Intermediate filaments are often disrupted by microtubule-targeting agents (14,15), although no specific binding sites for these agents have been identified on intermediate filaments. Previous studies have demonstrated the involvement of intermediate filaments, in particular cytokeratins, in acquired resistance to tubulin-binding agents such as paclitaxel (16), docetaxel (17), vincristine (18), and colcemid (18). Whether aberrations in other members of the intermediate filament proteins confer resistance to antimicrotubule agents is not known. In consideration of the significant role of vimentin in microtubule function (3), cell division (5), and cell signaling (5), elucidation of the involvement of vimentin in cancer cell resistance will be important for helping circumvent microtubule-targeting drug resistance in chronic cancer chemotherapy.

Peloruside A (PLA) and laulimalide (LAU) are two effective marine sponge-derived stabilizers of microtubules that inhibit cancer cell proliferation at low nanomolar concentrations (19,20). Although their mode of action is similar to that of the clinically useful anticancer drugs, paclitaxel (PTX) and the epothilones, PLA and LAU differ from them in terms of their binding site on β -tubulin, thus representing the only known class of non-taxoid site microtubule stabilizing agents (21–23). PLA and LAU retain their bioactivity in PTX- and epothilone-resistant cancer cells in which the taxoid site is mutated (22,23). Another advantage of PLA and LAU is that they show low susceptibility to the P-gp drug efflux pump compared to PTX and vinblastine (22,23).

Two drug-resistant human ovarian cancer cell lines are available in our lab for studying mechanisms of resistance to PLA and LAU, 1A9-R1 (R1) and 1A9-L4 (L4) cells derived from the parental 1A9 cell line (21). The R1 cells are 6-fold resistant to PLA but remain sensitive to LAU; whereas, the L4 cells are 39-fold resistant to both PLA and LAU. Importantly, the R1 and L4 cells remain sensitive to drugs that bind to the taxoid, vinca or colchicine sites on β -tubulin. Both resistant cell lines exhibit different single point-mutations in their β I-tubulin gene, and the L4 cells also have a high abundance of β II- and β III-tubulin isotypes

(21). The isotype alterations, however, play only a partial role in the resistance phenotype of L4 cells (24). The aim of the present study was to examine the proteome of the resistant cells using two-dimensional differential in-gel electrophoresis (2D-DIGE) to determine what other protein changes exist that might contribute to the resistance phenotype of the R1 and L4 cells.

MATERIALS AND METHODS

Cell Culture and Drugs

The 1A9 human ovarian carcinoma cell line and its drug-resistant sublines R1 (PLA-resistant), L4 (PLA/LAU-resistant), PTX-10 (PTX/epothilone-resistant) and 1A9-A8 (A8) (PTX/epothilone-resistant) were used in this study (21,25,26). Neither cell line was directly authenticated in our laboratory, but the cells retained their epithelial phenotype throughout the study. Cells were cultured in RPMI-1640 medium (Invitrogen, New Zealand) supplemented with 10% fetal calf serum (Invitrogen), 0.25 units/mL insulin (Sigma-Aldrich, New Zealand), 100 units/mL penicillin and 100 units/mL streptomycin (Invitrogen). The cells were maintained in a humidified incubator in a 5% CO₂-air atmosphere at 37°C.

PLA and LAU were isolated respectively from the marine sponges *Mycale hentscheli* (New Zealand) and *Cacospongia mycofijiense* (Tonga) (21), and stored as 1 mM stock solutions in absolute ethanol at –80°C. PTX was purchased from Sigma Chemical Company (New Zealand). Ixabepilone (IXA) was purchased from Bristol-Myers Squibb (Australia), and doxorubicin (DOX) was purchased from LC laboratories (Woburn, MA).

2D-DIGE

Cell lysate preparation and protein quantification were performed as previously described (21). The lysis buffer consisted of 30 mmol/L Tris-HCl (pH 8.8), 7 mol/L urea, 2 mol/L thiourea, and 4% (*w/v*) CHAPS, pH 8.5. As this buffer was hypotonic and would inhibit protease activity, no protease inhibitors were included in the buffer. Three independent lysates were prepared from each cell line. The pH of the cell lysates was checked by spotting 3 μ L lysate on a pH indicator strip, adjusted to pH 8.5 by adding 1.5 M Tris, pH 8.8, before labeling with Cy Dyes. Cy Dyes (GE Healthcare, Bucks, UK) were prepared to a working stock of 200 pmol/ μ L with high grade N,N-dimethylformamide (Sigma Chemical Co., Australia). For CyDye labeling, 10 μ g protein was incubated with 80 pmol of CyDye for 30 min at room temperature. The reaction was stopped by adding 10 mM lysine (1 μ L), then incubating for 10 min on

ice in the dark. The samples were randomly labeled with Cy3 or Cy5 to minimize potential dye artifacts (Table I). Additionally, an internal standard was generated by pooling equal amounts of proteins from every sample used in the experiment and labeling with Cy2 to provide a quantitative comparison between gels and to limit technical variation (Table I). The CyDye labeled proteins were mixed with rehydration buffer to give a total volume of 125 μ L, and the IPG strips (pI 3–5.6; length: 7 cm) were rehydrated with sample overnight in 3 mL of PlusOne dry strip cover fluid (GE Healthcare, New Zealand). Isoelectric focusing was conducted in an Ettan IPGphor Isoelectric Focusing Unit (GE Healthcare) with the following settings: (i) step and hold 300 V for 30 min; (ii) gradient 1,000 V for 30 min; (iii) gradient 5,000 V for 90 min; and (iv) step and hold 5,000 V for 25 min. After the isoelectric focusing, the strips were equilibrated in equilibration buffer (50 mmol/L Tris, 6 mol/L urea, 30% glycerol, and 2% SDS) containing 1% DTT for 10 min, then in equilibration buffer containing 2.5% iodoacetamide for 10 min. The second dimension was conducted on a 4% to 12% gradient NuPage Bis-Tris gel (Invitrogen) for 55 min at 200 V. The gels were scanned in a Fujifilm FLA-5100 imaging system (Fuji Photo Film Co., Ltd, Tokyo, Japan) using a 473 nm laser and a BPB1/530DF20 emission filter for Cy2, a 532 nm laser and a PBG/570DF20 emission filter for Cy3, and a 635 nm laser and a DBR1/R665 emission filter for Cy5 labelled proteins.

Analysis of Protein Expression

To analyse the expression profile of proteins in the 2D-DIGE gels, DeCyder™ 2D 6.5 software (GE Healthcare) was used. The biological variation analysis (BVA) module was used to match spots and calculate spot volumes. A master gel was created to automatically match and compare major spots between the gels based on the internal standards. Tests for significance were performed using the Student's *t*-test in the BVA module, and *P*-values ≤ 0.05 were considered significant.

MALDI-TOF Mass Spectrometry

To prepare selected protein spots for subsequent identification by MALDI-TOF mass spectrometry, a sample containing

80 μ g of protein was separated by two-dimensional electrophoresis as described in the 2D-DIGE protocol, and the gels were fixed in 2% phosphoric acid/50% ethanol (*v/v*) overnight and washed 3 times (each wash of 30 min) in double-distilled water (ddH₂O). The gel was incubated with staining solution (34% methanol, 17% ammonium sulfate, 3% phosphoric acid) for 1 h before adding 0.06% Coomassie® Brilliant blue G-250 (Biorad Laboratories, New Zealand) to the solution, and incubated for at least 2 days at room temperature with rocking. After washing the gels 3 times in ddH₂O, the spots were picked manually and subjected to an Ettan Automatic Digester (GE Healthcare) for tryptic digestion of the proteins. The digested peptides were recovered and spotted onto a MALDI plate and allowed to air dry overnight. MALDI-TOF analysis was performed using a Voyager-DE PRO mass spectrometer (Applied Biosystems, Foster City, CA). The peptide masses were calibrated using internal trypsin peaks, and the peptide mass maps were searched against the human NCBI database (v.7 November 2007; 5,614,267 sequences) using ProFound version 2002.03.01 online software provided by Rockefeller University, New York.

Western Blotting

The abundance of vimentin in the parental and the resistant cells was determined by Western blotting as described previously (21). A rabbit polyclonal primary antibody to vimentin (1:1000, ab45939, Abcam) and a Cy5-conjugated anti-rabbit secondary antibody (1:2500, PA45012V, GE Healthcare) were used to examine vimentin. A mouse monoclonal β -actin antibody (1:3,000, A2228, Sigma) was used as a loading control using a Cy5-conjugated anti-mouse secondary antibody (1:2,500; PA45010V, GE Healthcare). Band density was determined using ImageJ software from NIH. Vimentin abundance was presented as a percentage of the actin loading control.

Immunocytochemistry

Immunocytochemistry and confocal microscopy of the cells were performed as described previously (24). A rabbit polyclonal primary antibody to vimentin (1:1000, ab45939, Abcam) and an Alexa Fluor 488-conjugated antirabbit secondary antibody (1:1000, A11008, Invitrogen) were used.

Vimentin cDNA Transfection

Human transfection-ready vimentin cDNA (NM_003380) was purchased from Origene (Rockville, MD). The L4 cells were transfected with the vimentin cDNA using Lipofectamine 2000 reagent (Invitrogen) following the manufacturer's instructions. Briefly, the cells were seeded into wells of a 12-well cell culture plate and allowed to attach for 24 h, then

Table I Randomised CyDye Labeling Design for DIGE Experiments

Gel number	Cy3	Cy5	Cy2 (internal standard)
1	IA9 (lysate 1)	R1 (lysate 1)	Pool of all 9 samples
2	IA9 (lysate 2)	L4 (lysate 1)	Pool of all 9 samples
3	R1 (lysate 2)	IA9 (lysate 3)	Pool of all 9 samples
4	L4 (lysate 2)	R1 (lysate 3)	Pool of all 9 samples
5	L4 (lysate 3)	–	Pool of all 9 samples

transfected with vimentin cDNA for 12 h. The medium in the plates was replaced with complete cell culture medium, and the plate was incubated for an additional 36 h before being processed for protein quantification. The optimal cDNA concentration that gave high vimentin expression, but caused minimal cytotoxicity, was selected by transfecting L4 cells with varying concentrations (2 µg/well, 4 µg/well or 6 µg/well) of the cDNA. A Lipofectamine-only control (mock control) was also paired with each transfection experiment.

Cell Proliferation Assay

After 24 h cDNA transfection, the L4 cells were harvested and transferred to a 96-well culture plate (10,000 cells/well) and cultured for 24 h. The cells were then treated with PLA or LAU for 72 h, and cell proliferation was measured by MTT (3-(4,5-dimethylthiazol-2-yl)-2,5-diphenyltetrazolium bromide) assay. The IC₅₀ values of the drugs were obtained from a graph of percentage cell survival *versus* drug concentration using Sigma Plot software version 8 (Systat Software Inc., Point Richmond, CA).

Drug-Induced Vimentin Degradation

1A9 cells (5×10^5) were seeded into a 24-well plate and allowed to attach for 24 h. The cells were then treated with either 5 nM or 50 nM microtubule stabilizing or DNA damaging agents for 24 h and processed for Western blotting to determine the drug-induced degradation of vimentin protein.

RESULTS

Differential Protein Expression Profiles in PLA- and LAU-Resistant Cells

Intermediate filament proteins have been subdivided into several groups based on their homology; however, there is only a slight variation in their pI values, ranging from pI 4.5 to 5.6. In the present study, we performed 2D-DIGE to compare differentially expressed proteins in the pI range of 3 to 5.6, primarily to focus on the abundance of intermediate filament proteins in the PLA- and LAU-resistant R1 and L4 cells compared to parental 1A9 cells. A mixed internal standard enabled us to normalize spot volumes from each sample to perform gel-to-gel comparisons and to recognize statistically significant inter-spot variations. On each 2D gel, approximately 100 spots corresponding to proteins with a pI between 3 and 5.6 and a molecular weight between 10 and 250 kDa were detected and matched across 5 gels. Only a total of 8 spots showed statistically significant differences (P -value ≤ 0.05 , Student's *t*-test) in protein abundance between the parental and the resistant cell lines (Fig. 1), and these spots

were selected for MALDI identification. Six spots were downregulated in L4 cells, and two spots were upregulated compared to both the parental 1A9 and the resistant R1 cells. In the R1 cell line, among the 8 spots identified by MALDI, only two proteins showed a statistically significant change in abundance from the parental cells, one being upregulated and the other downregulated. The characteristics of each of the 8 different proteins are presented in Tables II and III.

Downregulation of Vimentin in PLA- and LAU-Resistant Cells

In order to further validate the vimentin changes that were identified by 2D-DIGE and MALDI-TOF, Western blotting and immunocytochemistry were performed. The 2D-DIGE protein profile of vimentin revealed a 1- and 13-fold decrease in its abundance in R1 and L4 cells, respectively, compared to the parental 1A9 cells (Fig. 1; Table III). Validation of vimentin expression by Western blotting confirmed that the protein was significantly downregulated in L4 cells (Fig. 2a and b). However, no significant change in the expression of vimentin in PLA-resistant R1 or PTX/epothilone-resistant PTX-10 or A8 cells was observed compared to 1A9 cells (Fig. 2a and b). Immunocytochemistry gave similar results with almost no vimentin fluorescent staining in the majority of the L4 cells; however, a small population of L4 cells was positive for vimentin expression, but the intensity of expression was much reduced compared with 1A9 and the other resistant cells (Fig. 2c).

Vimentin Transfection Sensitizes L4 Cells to PLA and LAU

To determine the role of vimentin in the sensitivity of L4 cells to PLA and LAU, L4 cells that express vimentin were generated by transiently transfecting a human vimentin cDNA into the cells. A final concentration of 2 µg/well, which gave ~60% of the 1A9 vimentin protein expression level, was used for all transfections (Fig. 3). Although higher cDNA concentrations (4 µg/well and 6 µg/well) were also tested, no further increase in vimentin expression was seen beyond 60% (Fig. 3). Moreover, there was no significant change in the expression level over 5 days (120 h) of transfection. To assess whether acquisition of vimentin expression influences the sensitivity of L4 cells to PLA and LAU, the ability of the drugs to inhibit proliferation of the transfected cells was tested using an MTT assay. The IC₅₀ values determined from the concentration-response curves showed that the cells transfected with vimentin cDNA were significantly more sensitive compared to the mock control-transfected L4 cells (Table IV). PLA sensitivity was increased by 21% ($P < 0.001$, $n = 4$) following vimentin transfection and LAU sensitivity was increased by 17% ($P < 0.01$, $n = 3$).

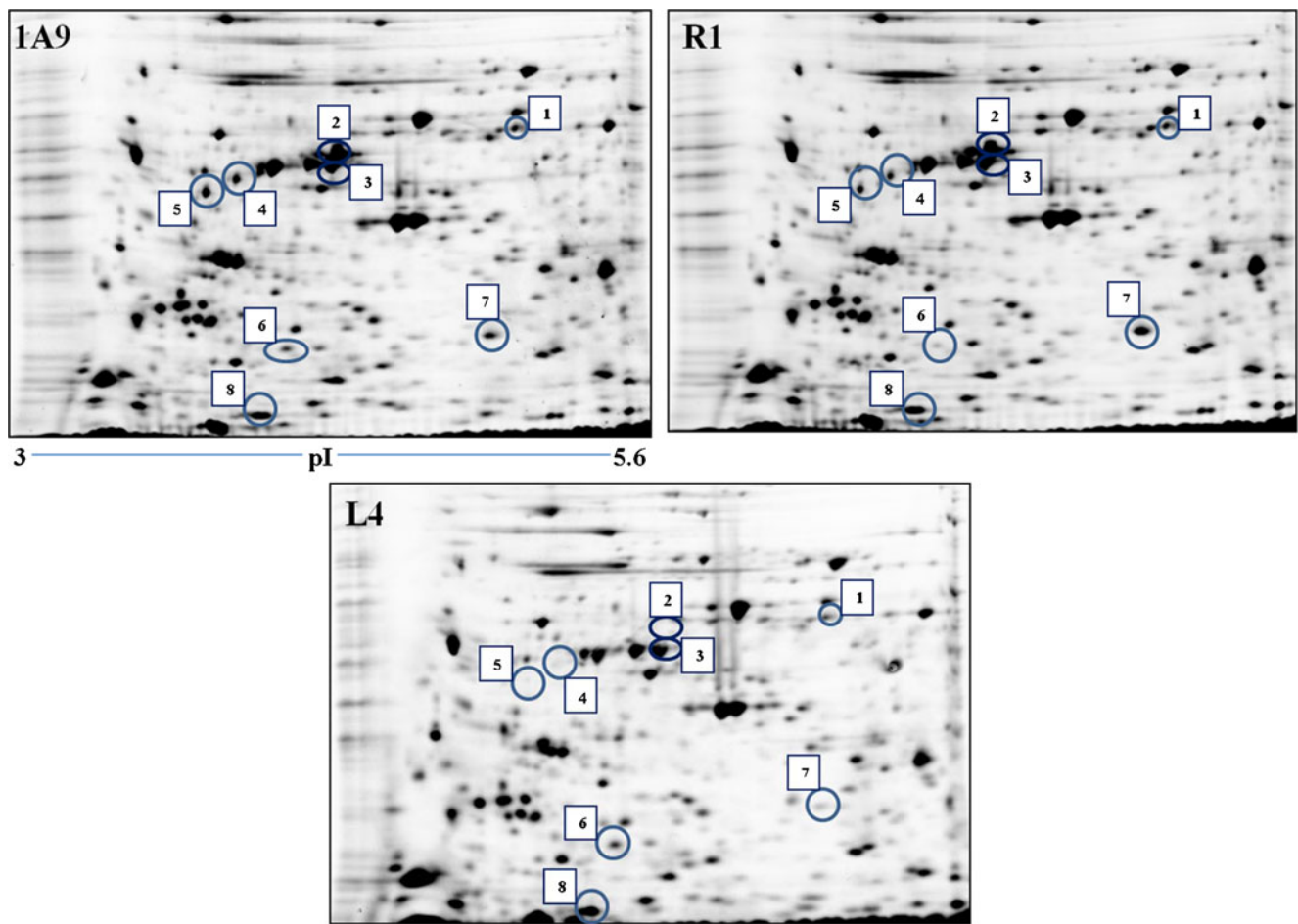


Fig. 1 2D-DIGE of IA9, R1 and L4 cells. Differentially expressed proteins in the resistant R1 and L4 cells compared to parental IA9 cells are circled. Each spot is numbered (squares) to match the data in Table II. Each image is representative of three independent preparations.

Chemotherapeutic Drugs Induce Vimentin Degradation

To determine whether PLA, LAU, and other chemotherapeutic drugs have any effect on either the expression or

metabolism of vimentin intermediate filament protein, parental IA9 cells were treated with various concentrations of the drugs for 24 h, and vimentin was examined by Western blotting. As shown in Fig. 4a, treatment with microtubule stabilizing agents as well as a DNA damaging agent resulted

Table II Differentially Expressed Proteins Identified by MALDI-TOF

Spot No. ^a	Protein name ^b	NCBI accession no.	Mol mass/pI Theoretical	Profound expectation	Sequence coverage (%)
1	Heat shock 70 kDa protein 9 precursor	gi 24234688	73.95/5.9	8.9×10^{-6}	22
2	Vimentin	gi 55977767	53.69/5.1	3.1×10^{-3}	46
3	α -Tubulin	gi 57013276	50.82/4.9	0.029	29
4	Vimentin (fragment)	gi 55977767	53.69/5.1	0.083	46
5	Vimentin (fragment)	gi 55977767	53.69/5.1	4.4×10^{-8}	63
6	Glyoxalase I chain A	gi 2392338	20.86/5.1	0.035	24
7	Creatine kinase M (fragment)	gi 180576	43.26/6.6	0.043	20
8	Elongin B isoform A	gi 6005890	13.23/4.7	0.017	20

^a Spot number represents the number given in the squares in Fig. 1

^b Proteins were identified by MALDI-TOF from selected spots of Coomassie blue-stained gels. Peptide mass fingerprinting for protein identification was performed using Profound's (v.2002.03.01) NCBI/nr human database (v.7 November 2007; 5614267)

Table III Fold Change of Differentially Expressed Proteins Between IA9, R1, and L4 Cells

Spot No.	Protein name	Fold change (IA9 vs R1) ^b	P-value ^a	Fold change (IA9 vs L4) ^b	P-value	Fold change (R1 vs L4) ^b	P-value
1	Heat shock 70 kDa protein 9 precursor	-1.15	0.21	-1.68	0.001	-1.46	0.038
2	Vimentin	-1.05	0.94	-13.66	0.001	-12.95	0.0002
3	α -Tubulin	1.02	0.78	-1.94	0.025	-1.98	0.023
4	Vimentin (fragment)	-1.19	0.64	-7.23	0.002	-6.08	0.002
5	Vimentin (fragment)	-1.32	0.35	-7.17	0.013	-5.45	0.019
6	Glyoxalase I chain A	-1.94	0.01	2.51	0.083	4.89	0.017
7	Creatine kinase M (fragment)	2.05	0.04	-8.24	0.007	-2.71	0.0008
8	Elongin B isoform A	1.1	0.3	2.08	0.014	2.35	0.019

^a Statistical analysis was carried out using the Student's *t*-test in the BVA (Biological Variation Analysis) module ($n=3$). $P \leq 0.05$ was taken as significant

^b Negative values represent downregulation in R1 or L4 cells compared to parental IA9 cells. In the comparison between R1 and L4, negative values represent downregulation in L4 cells

in the degradation of parental vimentin (M_r 58 kDa) into fragments of lower molecular weight. No vimentin degradation products (VDP) were seen in untreated IA9 cells. Importantly, the different compounds had a different concentration-dependent effect on vimentin degradation,

with 5 nM drug giving strong, intense VDP bands for PLA, LAU, and DOX and less dense bands for PTX and IXA; whereas, 50 nM drug reduced the intensity of the VDP bands relative to 5 nM drug for PLA, LAU, and DOX, but increased the intensity for PTX and IXA (Fig. 4a and b).

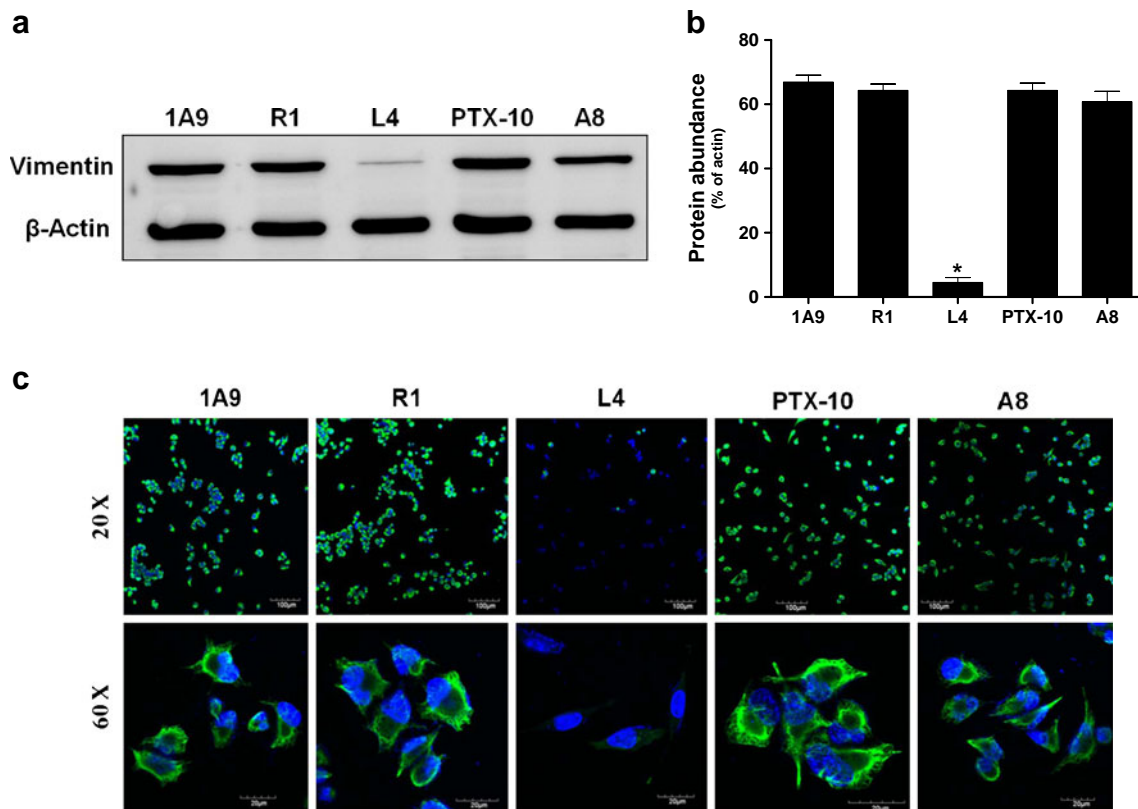
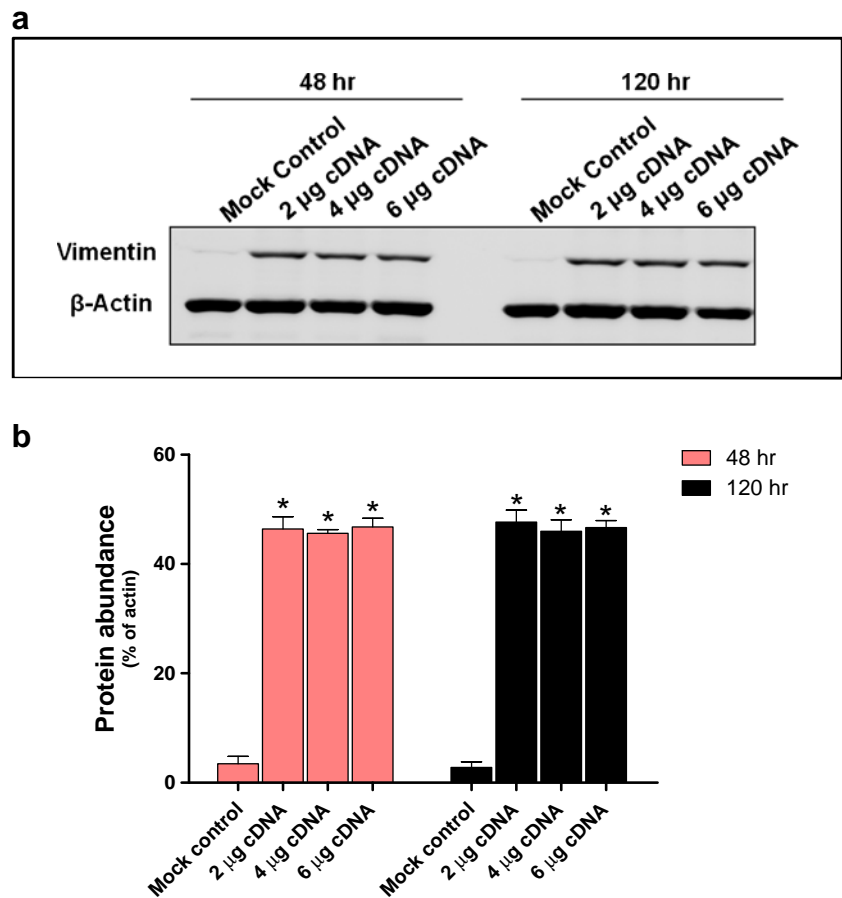


Fig. 2 Western blot and immunocytochemical analysis of vimentin in drug-resistant cells. **(a)** Cell lysates were prepared and subjected to electrophoresis and Western blotting. Actin was used as a loading control. A representative Western blot image is shown from 4 independent experiments. **(b)** Summary of vimentin protein abundance. Quantitation of immunoblot density was determined as % of actin loading control. Data are the mean \pm SEM of 4 independent experiments. $*P < 0.0001$, Student's *t*-test. **(c)** Immunocytochemistry of parental and the resistant cells. The cells were visualized by confocal microscopy using either 20x (top panel; scale bar=100 μ m) or 60x (bottom panel; scale bar=20 μ m) objectives. Only L4 cells show low vimentin abundance, supporting the Western blot results.

Fig. 3 Vimentin protein abundance in vimentin cDNA-transfected L4 cells. L4 cells were transfected with three vimentin cDNA concentrations or Lipofectamine on its own (mock control), and the protein abundance was determined by Western blot after 48 h and 120 h transfection. A representative blot from 3 independent experiments is shown in (a). Actin was used as a loading control. (b) A summary of the results is given in (b). Vimentin band densities are presented as % of actin loading control. The expression of vimentin-transfected cells is compared with the mock control-transfected cells. Data are the mean \pm SEM. * $P < 0.0001$, One-way ANOVA with Bonferroni multiple comparison test, $n=3$ experiments.



DISCUSSION

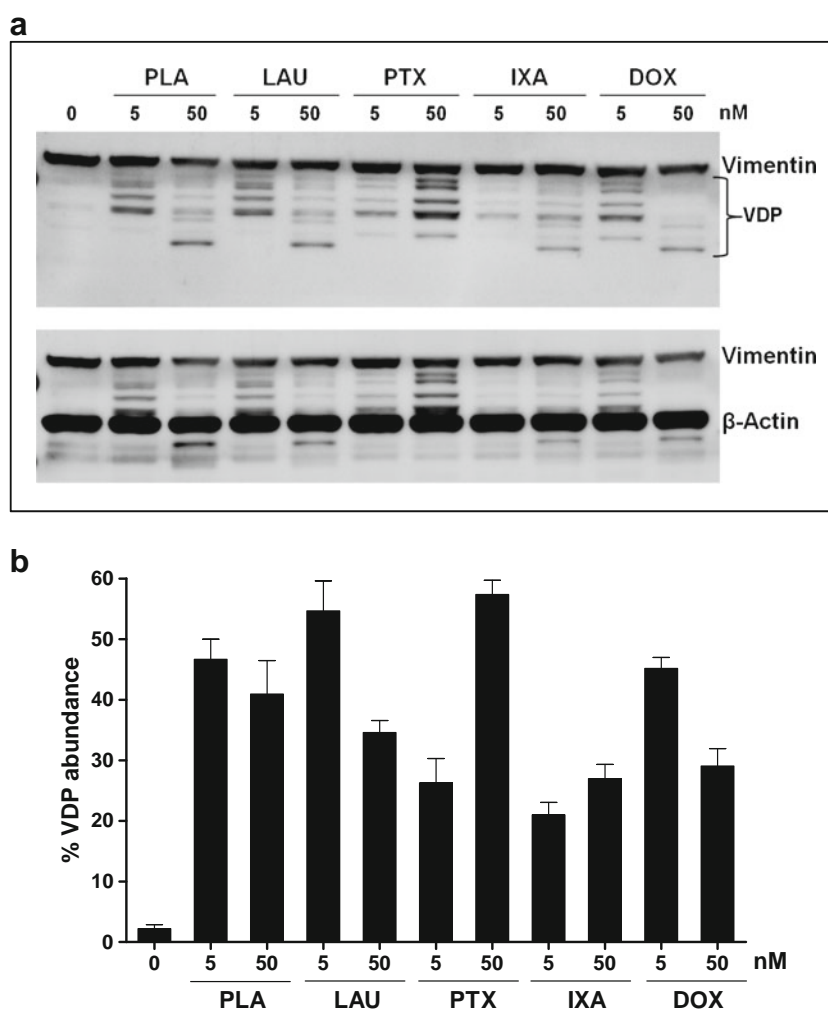
The present study using 2D-DIGE showed that two proteins (glyoxalase I and creatine kinase M) in R1 cells and five proteins (vimentin plus two vimentin fragments, heat shock protein 70, α -tubulin, creatine kinase M, and elongin B isoform A) in L4 cells were significantly altered relative to the parental 1A9 cells. Although the narrow pI range used in this study is a major limitation to drawing a general conclusion about the global-scale proteomics of the cells, many of the proteins identified here have not previously been shown to play a role in drug resistance. Therefore, this study introduces potential new mechanisms by which cancer cells may become resistant to antimicrotubule agents. The abundance of α -tubulin in the parental and the resistant cells was validated by Western blotting in a previous study (21). There was no significant alteration in the expression level of α -tubulin between parental 1A9 and the resistant R1 and L4 cells (21). This was anticipated since only a minor decrease (1.9-fold) in the protein level was identified by 2D-DIGE in the L4 cells compared to 1A9 cells. Proteins that showed less than a 2-fold alteration in their abundance by DIGE were not validated in the present study, including the creatine kinase M spot, which was only a fragment of the total protein. Vimentin abundance decreased 13-fold in L4

cells, and this significant downregulation was confirmed by Western blotting and immunocytochemistry. The observed vimentin alteration was unique to PLA/LAU-resistant L4 cells, and was not seen in R1 cells. Neither of the two taxoid drug-resistant cells had changes in their vimentin abundance either (Fig. 2). The functional significance of vimentin downregulation in the PLA and LAU sensitivity was, therefore, directly tested by transfecting a vimentin cDNA into L4 cells to restore a more normal vimentin abundance level. The acquisition of vimentin expression in L4 cells significantly restored some of their sensitivity to PLA and LAU by 1.2-fold compared to the vimentin-deficient mock control- or non-transfected cells (Table IV). It is believed that several mechanisms act together in drug resistance and each of these has a different effect on the resistance phenotype. Possible resistance mechanisms due to vimentin changes are discussed below. Given that L4 cells also have structural alterations in the primary drug target, β I-tubulin (21), it is likely that the majority of the resistance is a result of these changes in β -tubulin.

Tubulin-Targeted Drug Resistance due to Vimentin Alterations

There is no evidence to date of a direct involvement of vimentin in contributing to the resistance to antimicrotubule

Fig. 4 Drug-induced vimentin degradation in IA9 cells. **(a)** Treatment with 5 and 50 nM PLA, LAU, PTX, IXA, or DOX, individually, for 24 h led to vimentin degradation. For better visualization of vimentin degradation products (VDP), the transfer membrane is shown before staining for the actin loading control (top panel). The bottom panel shows the same transfer membrane with actin staining included. The image is representative of 3 independent experiments. **(b)** Summary of % VDP in drug-treated IA9 cells compared to non-degraded parental vimentin ($n=3$ independent experiments). The VDP abundances for all the drug-treated cells were significantly higher than that of untreated IA9 cells ($P < 0.001$, One-way ANOVA with Bonferroni's multiple comparison test). For LAU and PTX only, the % VDP of 5 nM versus 50 nM was also significant ($P < 0.05$). Data are the mean \pm SEM.



agents, despite the aforementioned associations between microtubules and vimentin. Previous studies, however, have reported that vimentin-negative cells increase their expression of vimentin after selection for resistance to tubulin-

Table IV IC₅₀ Values for PLA and LAU in Vimentin-Transfected L4 Cells

Drugs	L4 (IC ₅₀ nmol/L) ^a		
	Non-transfected control	Mock control	Vimentin-transfected cells
PLA	326.0 \pm 3.4	331.8 \pm 6.6 (0.98-fold) ^b	261.5 \pm 6.3** (1.26-fold) ^c
LAU	262.8 \pm 4.4	258.2 \pm 6.5 (1.01-fold) ^b	215.6 \pm 6.0* (1.19-fold) ^c

^a The IC₅₀ values of PLA and LAU in vimentin cDNA-transfected L4 and control cells were determined by MTT assay. Data are presented as the mean \pm SEM of 3–4 independent experiments. * $P < 0.01$, ** $P < 0.001$, Student's *t*-test

^b The fold changes in resistance in mock-transfected cells to non-transfected cells

^c The fold changes in resistance in vimentin-transfected cells compared to mock-transfected cells. A value of 1 indicates no change, and a value of > 1.0 indicates an increased sensitivity to the drug

binding agents. For example, human cancer cells selected for resistance to PTX and docetaxel show increased abundance of vimentin compared to the non-resistant cells (27,28). This is the exact opposite to the resistant L4 cells in the present study that showed a large decrease in vimentin relative to the sensitive IA9 cells. Since the actual mechanism by which vimentin confers drug resistance to cancer cells has not yet been elucidated, the significance of these vimentin alterations is unknown, but it has been postulated that vimentin may have effects due to its close association with microtubules (3,29). This is further supported by the fact that the phosphorylation status and distribution of vimentin is altered by PTX-treatment in normal and cancer cells (15,16,30).

A number of other studies have provided evidence for a role of vimentin in several cell signaling networks (5). Vimentin contains multiple phosphorylation sites and is an important substrate for a number of kinases, including Rho kinase, protein kinase C, cGMP kinase, Yes kinase, Raf-1 kinase, PAK kinase, and Aurora B kinase that are involved in a variety of key cellular functions, including signal transduction, cell division, and apoptosis (5,31–33). Recently, the

PI3K/Akt cell survival pathway has been shown to mediate vimentin expression (34). Vimentin also regulates 14-3-3 proteins, which play a vital role in cell signaling and cell cycle processes (35). In one study on resistant human colon cancer cells, overexpression of vimentin reduced the anti-apoptotic effect of Bcl-2, causing an increase in apoptosis induced by methotrexate; whereas, downregulation of vimentin caused a decrease in apoptosis (36). Protection from apoptosis is a well known way for cells to display resistance to drugs (37). In another study in c-erbB-2 oncogene overexpressing breast cancer tumors that are known to be refractory to diverse chemotherapies, underexpression of vimentin was identified (38). Our study shows that vimentin is downregulated in a cell line (L4) that is highly resistant to PLA and LAU. Considering the involvement of vimentin in various cell signaling processes that interact with a large number of cellular proteins, it is possible that decreased vimentin abundance in L4 cells may lead to alterations in signaling pathways that regulate cell survival or apoptosis, thereby conferring resistance to PLA and LAU, both of which are known to cause apoptosis (19,39).

Drug-Induced Vimentin Cleavage and Apoptosis

Cytoskeletal reorganization is a characteristic feature of apoptosis induced by diverse cytotoxic drugs (14). A study by Grzanka *et al.* (15) using fluorescence microscopy showed that treatment with PTX, etoposide, or DOX resulted in accumulation of vimentin at the site of apoptotic bodies in human leukemic K-562 and HL-60 cells. In these cells, PTX-treatment caused the expected effects on microtubules but also induced significant changes in the distribution of vimentin, with a thin network of vimentin dispersed throughout the cells and nucleus or aggregated in apoptotic bodies (15). Using an *in vitro* model system of human prostate epithelial cells, Prasad *et al.* (40) demonstrated that proteolysis of vimentin is associated with the execution phase of apoptosis induced by ionizing radiation. Caspases play a vital role in the execution of apoptosis by cleaving or activating diverse intracellular proteins. A caspase-mediated cleavage of vimentin is a major event during apoptosis and contributes to the morphological changes that characterize apoptotic cells (41). Moreover, the degradation of vimentin by caspases promotes apoptosis by disrupting intermediate filaments and amplifying the cell death signal through a pro-apoptotic N-terminal cleavage product (42). Withaferin-A, a naturally derived bioactive compound, is believed to target vimentin, since withaferin-A cleaves vimentin and causes marked apoptosis in vimentin-expressing tumor cells but leads to significantly less apoptotic damage in vimentin-deficient tumor cells (43). Knockdown of vimentin expression or inhibition of caspase-induced vimentin degradation abrogated apoptosis in these cells. In our study, both

microtubule stabilizing agents and a DNA-damaging agent that are known to induce apoptosis caused vimentin degradation in vimentin-expressing 1A9 cells (Fig. 4). Although PTX and DOX have already been shown by others to disrupt the vimentin network, this is the first study demonstrating degradation of vimentin in mammalian cells in response to PLA, LAU and IXA. It is unclear why a major downregulation of vimentin does not affect sensitivity of L4 cells to PTX, IXA, and DOX, in addition to PLA and LAU. A number of cellular processes are affected by microtubule-targeting agents as a result of their molecular interaction with microtubules and also their interaction with several other secondary targets, which may or may not be similar between different tubulin-binding agents. Supporting this fact, PLA and PTX have previously been shown to affect different apoptotic proteins in human HL-60 promyeloid leukemic cells (44). Given the role played by vimentin in apoptosis in other cells (40–43), our results suggest that drug interactions with vimentin or vimentin cleavage to VDP might be vital for regulating the apoptotic signaling pathways specifically activated by PLA and LAU. This might in part explain the specific resistance of L4 cells to PLA and LAU, but not to other tubulin-binding agents (21). However, further investigations are necessary to better understand the role of vimentin in cell survival pathways and in mediating the sensitivity to tubulin-binding antimetabolic agents.

CONCLUSION

We have identified a novel mechanism of resistance to PLA and LAU that involves the downregulation of vimentin. Since, there is little detailed information available on the link between antitubulin drug resistance and vimentin abundance in cancer cells, the information provided here may offer some reasonable insights on vimentin-mediated resistance mechanisms in cancer cells with regard to antimicrotubule agents like the microtubule stabilizing drugs. The finding that decreased vimentin expression in L4 cells is associated with resistance to non-taxoid, non-vinca, and non-colchicine site directed microtubule-targeting agents indicates that the role of vimentin in acquisition of resistance is complex, and that this effect may be linked to the mode of induction of cell-death by these agents.

ACKNOWLEDGMENTS AND DISCLOSURES

The authors thank Dr. Paraskevi Giannakakou for kindly providing the 1A9 and the resistant L4, PTX-10, and A8 cell lines. This research was supported by grants to J.H.M from the Cancer Society of New Zealand, the Wellington Medical Research Foundation, and Victoria University of Wellington.

REFERENCES

- Steinert PM, Roop DR. Molecular and cellular biology of intermediate filaments. *Annu Rev Biochem.* 1988;57:593–625.
- Franke WW, Schmid E, Winter S, Osborn M, Weber K. Widespread occurrence of intermediate-sized filaments of the vimentin-type in cultured cells from diverse vertebrates. *Exp Cell Res.* 1979;123(1):25–46.
- Dráberová E, Dráber P. A microtubule-interacting protein involved in coalignment of vimentin intermediate filaments with microtubules. *J Cell Sci.* 1993;106(4):1263–73.
- Esue O, Carson AA, Tseng Y, Wirtz D. A direct interaction between actin and vimentin filaments mediated by the tail domain of vimentin. *J Biol Chem.* 2006;281(41):30393–9.
- Satelli A, Li S. Vimentin in cancer and its potential as a molecular target for cancer therapy. *Cell Mol Life Sci.* 2011;68(18):3033–46.
- Zhu QS, Rosenblatt K, Huang KL, Lahat G, Brobey R, Bolshakov S, *et al.* Vimentin is a novel AKT1 target mediating motility and invasion. *Oncogene.* 2011;30(4):457–70.
- Nijkamp MM, Span PN, Hoogsteen IJ, van der Kogel AJ, Kaanders JH, Bussink J. Expression of E-cadherin and vimentin correlates with metastasis formation in head and neck squamous cell carcinoma patients. *Radiother Oncol.* 2011;99(3):344–8.
- Liang Y, McDonnell S, Clynes M. Examining the relationship between cancer invasion/metastasis and drug resistance. *Curr Cancer Drug Targets.* 2002;2(3):257–77.
- Dumontet C, Jordan MA. Microtubule-binding agents: a dynamic field of cancer therapeutics. *Nat Rev Drug Discov.* 2010;9(10):790–803.
- Gottesman MM, Fojo T, Bates SE. Multidrug resistance in cancer: role of ATP -dependent transporters. *Nat Rev Cancer.* 2002;2(1):48–58.
- Kavallaris M. Microtubules and resistance to tubulin-binding agents. *Nat Rev Cancer.* 2010;10(3):194–204.
- Verrills NM, Po'uha ST, Liu ML, Liaw TY, Larsen MR, Ivery MT, *et al.* Alterations in gamma-actin and tubulin-targeted drug resistance in childhood leukemia. *J Natl Cancer Inst.* 2006;98(19):1363–74.
- Zhou M, Liu Z, Zhao Y, Ding Y, Liu H, Xi Y, *et al.* MicroRNA-125b confers the resistance of breast cancer cells to paclitaxel through suppression of pro-apoptotic Bcl-2 antagonist killer 1 (Bak1) expression. *J Biol Chem.* 2010;285(28):21496–507.
- Grzanka A, Grzanka D, Orlikowska M. Cytoskeletal reorganization during process of apoptosis induced by cytostatic drugs in K-562 and HL-60 leukemia cell lines. *Biochem Pharmacol.* 2003;66(8):1611–7.
- Grzanka A, Grzanka D, Orlikowska M, Zuryn A, Grzanka A. Estimation of taxol influence on changes in tubulin and vimentin systems in K-562 and HL-60 cell lines by immunofluorescence microscopy. *Neoplasma.* 2005;52(3):193–8.
- Sun QL, Sha HF, Yang XH, Bao GL, Lu J, Xie YY. Comparative proteomic analysis of paclitaxel sensitive A549 lung adenocarcinoma cell line and its resistant counterpart A549-Taxol. *J Cancer Res Clin Oncol.* 2011;137(3):521–32.
- Kabos P, Haughian JM, Wang X, Dye WW, Finlayson C, Elias A, *et al.* Cytokeratin 5 positive cells represent a steroid receptor negative and therapy resistant subpopulation in luminal breast cancers. *Breast Cancer Res Treat.* 2011;128(1):45–55.
- Bauman PA, Dalton WS, Anderson JM, Cress AE. Expression of cytokeratin confers multiple drug resistance. *Proc Natl Acad Sci U S A.* 1994;91(12):5311–4.
- Mooberry SL, Tien G, Hernandez AH, Plubrukarn A, Davidson BS. Laulimalide and isolaulimalide, new paclitaxel-like microtubule stabilizing agents. *Cancer Res.* 1999;59(3):653–60.
- Hood KA, West LM, Rouwé B, Northcote PT, Berridge MV, Wakefield SJ, *et al.* Peloruside A, a novel antimetabolic agent with paclitaxel-like microtubule stabilizing activity. *Cancer Res.* 2002;62(12):3356–60.
- Kanakkanthara A, Wilmes A, O'Brate A, Escuin D, Chan A, Gjyzezi A, *et al.* Peloruside- and laulimalide-resistant human ovarian carcinoma cells have β I-tubulin mutations and altered expression of β II- and β III-tubulin isoforms. *Mol Cancer Ther.* 2011;10(8):1419–29.
- Gaitanos TN, Buey RM, Díaz F, Northcote PT, Spittle PT, Andreu JM, *et al.* Peloruside A does not bind to the taxoid site on β -tubulin and retains its activity in multidrug-resistant cell lines. *Cancer Res.* 2004;64(15):5063–7.
- Pryor DE, O'Brate A, Bilcer G, Diaz JF, Wang Y, Wang Y, *et al.* The microtubule stabilizing agent laulimalide does not bind in the taxoid site, kills cells resistant to paclitaxel and epothilones, and may not require its epoxide moiety for activity. *Biochemistry.* 2002;41(29):9109–15.
- Kanakkanthara A, Northcote PT, Miller JH. β II-Tubulin and β III-tubulin mediate sensitivity to peloruside A and laulimalide, but not paclitaxel or vinblastine, in human ovarian carcinoma cells. *Mol Cancer Ther.* 2012;11(2):393–404.
- Giannakakou P, Sackett DL, Kang YK, Zhan Z, Buters JTM, Fojo T, *et al.* Paclitaxel-resistant human ovarian cancer cells have mutant β -tubulins that exhibit impaired paclitaxel-driven polymerization. *J Biol Chem.* 1997;272(27):17118–25.
- Giannakakou P, Gussio R, Nogales E, Downing KH, Zaharevitz D, Bollbuck B, *et al.* A common pharmacophore for epothilone and taxanes: molecular basis for drug resistance conferred by tubulin mutations in human cancer cells. *Proc Natl Acad Sci U S A.* 2000;97(6):2904–9.
- Kajiyama H, Shibata K, Terauchi M, Yamashita M, Ino K, Nawa A, *et al.* Chemoresistance to paclitaxel induces epithelial-mesenchymal transition and enhances metastatic potential for epithelial ovarian carcinoma cells. *Int J Oncol.* 2007;31(2):277–83.
- Işeri OD, Kars MD, Arpacı F, Atalay C, Pak I, Gündüz U. Drug resistant MCF-7 cells exhibit epithelial-mesenchymal transition gene expression pattern. *Biomed Pharmacother.* 2011;65(1):40–5.
- Goldman RD, Khuon S, Chou YH, Opal P, Steinert PM. The function of intermediate filaments in cell shape and cytoskeletal integrity. *J Cell Biol.* 1996;134(4):971–83.
- Vilalta PM, Zhang L, Hamm-Alvarez SF. A novel taxol-induced vimentin phosphorylation and stabilization revealed by studies on stable microtubules and vimentin intermediate filaments. *J Cell Sci.* 1998;111(13):1841–52.
- Janosch P, Kieser A, Eulitz M, Lovric J, Sauer G, Reichert M, *et al.* The Raf-1 kinase associates with vimentin kinases and regulates the structure of vimentin filaments. *FASEB J.* 2000;14(13):2008–21.
- Goto H, Tanabe K, Manser E, Lim L, Yasui Y, Inagaki M. Phosphorylation and reorganization of vimentin by p21-activated kinase (PAK). *Genes Cells.* 2002;7(2):91–7.
- Goto H, Yasui Y, Kawajiri A, Nigg EA, Terada Y, Tatsuka M, *et al.* Aurora-B regulates the cleavage furrow-specific vimentin phosphorylation in the cytokinetic process. *J Biol Chem.* 2003;278(10):8526–30.
- Nitta T, Kim JS, Mohuczy D, Behrens KE. Murine cirrhosis induces hepatocyte epithelial-mesenchymal transition and alterations in survival signaling pathways. *Hepatology.* 2008;48(3):909–19.
- Tzivion G, Luo ZJ, Avruch J. Calyculin A-induced vimentin phosphorylation sequesters 14-3-3 and displaces other 14-3-3 partners *in vivo*. *J Biol Chem.* 2000;275(38):29772–8.
- Peñuelas S, Noé V, Ciudad CJ. Modulation of IMPDH2, survivin, topoisomerase I and vimentin increases sensitivity to methotrexate in HT29 human colon cancer cells. *FEBS J.* 2005;272(3):696–710.

37. Lopes EC, García MG, Vellón L, Alvarez E, Hajos SE. Correlation between decreased apoptosis and multidrug resistance (MDR) in murine leukemic T cell lines. *Leuk Lymphoma*. 2001;42(4):775–87.
38. Wilson KS, Roberts H, Leek R, Harris AL, Geradts J. Differential gene expression patterns in HER2/neu-positive and -negative breast cancer cell lines and tissues. *Am J Pathol*. 2002;161(4):1171–85.
39. Miller JH, Rouwé B, Gaitanos TN, Hood KA, Crume KP, Bäckström BT, *et al*. Peloruside A enhances apoptosis in H-ras-transformed cells and is cytotoxic to proliferating T cells. *Apoptosis*. 2004;9(6):785–96.
40. Prasad SC, Thraves PJ, Kuettel MR, Srinivasarao GY, Dritschilo A, Soldatenkov VA. Apoptosis-associated proteolysis of vimentin in human prostate epithelial tumor cells. *Biochem Biophys Res Commun*. 1998;249(2):332–8.
41. Morishima N. Changes in nuclear morphology during apoptosis correlate with vimentin cleavage by different caspases located either upstream or downstream of Bcl-2 action. *Genes Cells*. 1999;4(7):401–14.
42. Byun Y, Chen F, Chang R, Trivedi M, Green KJ, Cryns VL. Caspase cleavage of vimentin disrupts intermediate filaments and promotes apoptosis. *Cell Death Differ*. 2001;8(5):443–50.
43. Lahat G, Zhu QS, Huang KL, Wang S, Bolshakov S, Liu J, *et al*. Vimentin is a novel anti-cancer therapeutic target; insights from *in vitro* and *in vivo* mice xenograft studies. *PLoS One*. 2010;5(4):e10105.
44. Wilmes A, Chan A, Rawson P, William Jordan T, Miller JH. Paclitaxel effects on the proteome of HL-60 promyelocytic leukemic cells: comparison to peloruside A. *Invest New Drugs*. 2012;30(1):121–9.